

Sensor Query Schedule and Sensor Noise Covariances for Accuracy-constrained Trajectory Estimation

Abhishek Goudar¹ and Angela P. Schoellig¹

Abstract—Trajectory estimation involves determining the trajectory of a mobile robot by combining prior knowledge about its dynamic model with noisy observations of its state obtained using sensors. The accuracy of such a procedure is dictated by the system model fidelity and the sensor parameters, such as the accuracy of the sensor (as represented by its noise covariance) and the rate at which it can generate observations, referred to as the sensor query schedule. Intuitively, high-rate measurements from accurate sensors lead to accurate trajectory estimation. However, cost and resource constraints limit the sensor accuracy and its measurement rate. Our work’s novel contribution is the estimation of sensor schedules and sensor covariances necessary to achieve a *specific estimation accuracy*. Concretely, we focus on estimating: (i) the rate or *schedule* with which a sensor of known covariance must generate measurements to achieve specific estimation accuracy, and alternatively, (ii) the sensor covariance necessary to achieve specific estimation accuracy for a given sensor update rate. We formulate the problem of estimating these sensor parameters as semidefinite programs, which can be solved by off-the-shelf solvers. We validate our approach in simulation and real experiments by showing that the sensor schedules and the sensor covariances calculated using our proposed method achieve the desired trajectory estimation accuracy. Our method also identifies scenarios where certain estimation accuracy is unachievable with the given system and sensor characteristics.

Index Terms—Localization, Probability and Statistical Methods, Optimization and Optimal control.

I. INTRODUCTION

THE task of estimating the trajectory of a mobile system involves determining its position (and orientation) over time as it moves through the environment. A common approach to do this is to combine prior knowledge about the system’s dynamics with measurements of the system’s state obtained using sensors. The accuracy of any such trajectory estimation method is governed by (i) the system model fidelity, and (ii) the accuracy and frequency of sensory measurements. The accuracy of an unbiased sensor is captured by its *sensor noise covariance* values, with lower covariance values implying higher accuracy. We refer to the frequency or schedule with

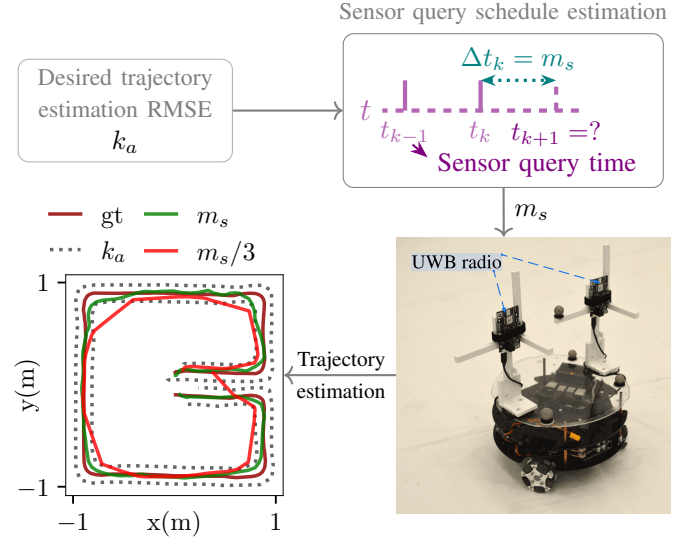


Fig. 1. Application of the proposed sensor query schedule calculation approach to trajectory estimation. For a desired trajectory estimation root mean square error (RMSE), we calculate a sensor query schedule using our proposed method (top right). The calculated query schedule is then used to generate measurements on our robot for use in the trajectory estimation pipeline (bottom right). Results from real experiments showing the estimated trajectory, using the proposed query rate m_s (optimal rate) and a lower query rate $m_s/3$ (suboptimal rate), the ground-truth (gt) trajectory, and the desired accuracy envelope (k_a) are shown (bottom left). The trajectory estimated with the proposed query rate is consistently within the accuracy envelope whereas the trajectory estimated using the lower query rate breaches the accuracy envelope on several instances, showing the validity of our approach.

which a sensor generates measurements as its *sensor query schedule*. It follows that querying sensors with lower covariance at higher frequencies will achieve better trajectory estimation accuracy. Various factors such as manufacturing cost, power consumption, communication bandwidth, and available compute restrict the accuracy (or covariance) of a sensor and the rate at which it can generate measurements. For example, we consider ultra-wideband (UWB) radios that operate in two-way ranging (TWR) mode [1]. In this mode, a robot equipped with a UWB radio (referred to as a *tag*) individually measures its distance to other UWB radios installed in the environment (referred to as *anchors*). Due to the high-bandwidth nature of UWB technology, only one UWB radio can transmit at any given time. Additionally, due to the finite time of flight delay [1], two UWB radios can only communicate up to a certain maximum measurement frequency. Hence, if a tag operates at its maximum measurement frequency, no other tag can acquire distance measurements. However, if the desired estimation accuracy can be achieved at a lower measurement frequency, then multiple tags can share the same channel. The overarching goal and contribution of our work is to estimate

Manuscript received: December, 23, 2024; Revised March, 19, 2025; Accepted May, 3, 2025.

This paper was recommended for publication by Editor Lucia Pallottino upon evaluation of the Associate Editor and Reviewers’ comments.

This work was supported in part by the Natural Sciences and Engineering Research Council of Canada (NSERC) and in part by the Canada CIFAR AI Chairs Program.

¹The authors are with the Learning Systems and Robotics Lab at the Technical University of Munich, Germany, and the University of Toronto Institute for Aerospace Studies, Canada. They are also affiliated with the University of Toronto Robotics Institute, the Munich Institute of Robotics and Machine Intelligence (MIRMI), and the Vector Institute for Artificial Intelligence. E-mail: abhishek.goudar@robotics.utoronto.ca, angela.schoellig@tum.de

Digital Object Identifier (DOI): see top of this page.

sensor parameters such as the sensor query schedule and the sensor noise covariances necessary to achieve a desired trajectory estimation accuracy.

An overview of our approach to sensor query schedule estimation is shown in Figure 1. For a desired trajectory estimation root mean square error (RMSE), we calculate the sensor query schedule using our proposed method (outlined in Section V-C). The calculated query schedule is then used to generate measurements for trajectory estimation.

Next, we highlight another benefit of our approach. A common criterion for selecting sensor parameters is to choose parameters that minimize the state uncertainty [2], [3]. However, such an approach cannot be used to determine if the desired estimation accuracy is achievable. Since our approach considers trajectory estimation accuracy explicitly, it can identify scenarios where certain estimation accuracy is infeasible given the system parameters. The following are the main contributions of our work:

- An estimator-agnostic optimization-based approach for calculating sensor parameters that incorporates the desired estimation accuracy.
- Application of the proposed framework to estimate (i) the sensor query schedule (for a given sensor noise covariance) and (ii) sensor noise covariance (for a given query schedule) for trajectory estimation.
- Evaluation of our methods in simulation and real experiments. We share our code used in the experiments ¹.

II. RELATED WORK

We review previous works that focus on sensor scheduling, sensor parameter estimation, and the achievable performance of estimators commonly used in state estimation for robotics. In probabilistic state estimation, a common approach for scheduling sensors in robotic systems is to optimize for sensor query frequencies that minimize the posterior state covariance estimator [2], [4]. Such an approach can yield low estimation error, but at the cost of injudicious use of sensory data. Our proposed method provides sensor query schedules optimized for a specific desired estimation accuracy, leading to judicious use of sensor measurements. An alternative approach to sensor scheduling is to trigger a measurement request when the estimated uncertainty of a particular estimator (the unscented Kalman filter (UKF)) is above a certain threshold [3]. Such an approach takes estimation uncertainty into account explicitly, but the calculated sensor schedule is specific to the employed state estimation method. In contrast, we use the posterior Cramér-Rao bound (PCRB) [5] to calculate estimator-agnostic sensor schedules that achieve the desired estimation accuracy. The PCRB can be viewed as a Bayesian analog of the parametric Cramér-Rao bound (CRB) [6], [7]. Unlike the CRB, the PCRB also holds for estimators with unknown bias under mild assumptions [8]. We also propose a *convex* SDP formulation for calculating sensor query schedules that can be solved efficiently using off-the-shelf solvers and can identify scenarios where certain estimation accuracy is infeasible.

The Fisher information matrix (FIM) [9] and CRB [6], [7] have been used in an array of problems such as the observability analysis of the simultaneous localization and mapping (SLAM) framework [10], planning for localization [11], and active perception [12]. The CRB has been used to derive bounds on the achievable localization accuracy in range-based positioning [13]. The CRB has also been applied to localization of transmitters from time-difference-of-arrival measurements [14], [15], choosing among multiple observations by exploiting their *submodular* (diminishing return property) nature [16], and simultaneous placement and scheduling of sensors [17]. More recently, the problem of optimal beacon placement for range-aided localization was formulated as maximization of a submodular set function based on the FIM [18]. In a related application, an information-theoretic objective is used to design optimal placement for a set of diverse sensors on a mobile robot for improved sensing [19]. The PCRB has been relatively less explored in robotics. A common application of the PCRB is to design a generic framework to deploy and schedule multisensor systems based on sensor contributions [20]. Since PCRB provides a lower bound on the estimation mean square error, it has been used to evaluate the effect of different sensing modalities for SLAM [21]. The previous approaches directly minimize the lower bounds provided by the CRB and the PCRB to estimate sensor placements and schedules, and do not consider the required estimation accuracy explicitly. Our proposed method calculates an estimator-agnostic sensor query schedule by minimizing the predictive PCRB that incorporates the required estimation accuracy explicitly.

Sensor covariances are typically identified using sensor data sheets or through an offline calibration procedure. An alternative approach is to estimate the sensor noise models online using a bi-level optimization approach. Specifically, covariances for robot motion and sensor models can be estimated using an expectation-maximization-based approach [22]. Alternatively, a data-driven approach can be used to estimate the process density of a motion prior using ground-truth information [23]. Similarly, sensor noise models can also be estimated using incremental maximum a posteriori inference [24]. More recently, [25] proposed a convex formulation for the problem of joint state and noise covariance estimation within the maximum a posteriori (MAP) inference framework. While these works proposed methods that estimate sensor covariances to improve trajectory estimation accuracy, our framework estimates sensor noise covariances required to achieve a specific estimation accuracy. As mentioned before, our proposed framework can also be used to identify if particular estimation accuracy is unachievable for a given sensor setup. To the best of the authors' knowledge, the calculation of sensor query schedules and sensor noise covariances that achieve a desired trajectory estimation accuracy has not been done before. In the next section we introduce the necessary background for our problem formulation.

III. PRELIMINARIES

We introduce the notation used in this paper. Lower-case symbols are used to represent scalar quantities. Bold lower-

¹https://github.com/abhigoudar/spi_acte

case and upper-case symbols are used to represent vectors and matrices, respectively. The set of positive real numbers is denoted by \mathbb{R}_{++} and the sets of $d \times d$ positive definite and positive semidefinite matrices are represented by \mathbb{S}_{++}^d and \mathbb{S}_+^d , respectively. For a matrix $\mathbf{A} \in \mathbb{R}^{d \times d}$, $\mathbf{A} \succcurlyeq 0$ implies $\mathbf{A} \in \mathbb{S}_+^d$, and $\mathbf{A} \succ 0$ implies $\mathbf{A} \in \mathbb{S}_{++}^d$. For matrices $\mathbf{A}, \mathbf{B} \in \mathbb{S}_+^d$, $\mathbf{A} \succcurlyeq \mathbf{B}$ implies $\mathbf{A} - \mathbf{B} \succcurlyeq 0$.

A. System model

We consider nonlinear systems of the form

$$\begin{aligned} \mathbf{x}_{k+1} &= f(\mathbf{x}_k, \mathbf{u}_k) + \mathbf{w}_k, \\ \mathbf{y}_k &= h(\mathbf{x}_k) + \boldsymbol{\eta}_k, \end{aligned} \quad (1)$$

where the subscript k represents the time index, \mathbf{x}_k is state at time t_k , \mathbf{u}_k is the control input, \mathbf{y}_k is the measurement obtained at time t_k , and $\mathbf{w}_k \sim \mathcal{N}(\mathbf{0}, \mathbf{Q}_k)$ and $\boldsymbol{\eta}_k \sim \mathcal{N}(\mathbf{0}, \mathbf{R}_k)$ are additive white Gaussian noise (AWGN) with covariances \mathbf{Q}_k and \mathbf{R}_k , respectively. The system process model is represented by the nonlinear function $f(\cdot)$ and the measurement model by $h(\cdot)$, respectively. We assume that the measurement noise, process noise, and the initial state, \mathbf{x}_0 , are uncorrelated with each other and over time.

B. Estimation error

The goal of a state estimator is to infer the state of a system by combining knowledge about the system model with noisy observations of the state obtained using sensors. To assess its performance, we can use the estimator *mean squared error* (MSE) as the metric. Let $g(\mathbf{y})$ be an estimate of the true state \mathbf{x} , then the estimator MSE is given by

$$\text{MSE}(\mathbf{x}) = \mathbb{E} \left[(g(\mathbf{y}) - \mathbf{x})(g(\mathbf{y}) - \mathbf{x})^T \right], \quad (2)$$

which is matrix-valued and considers both the (co)variance and the bias of an estimator [26, Section 8.2]. An estimate of the state can be obtained using a filtering or an optimization-based approach. We will refer to the matrix resulting from the expected outer product in (2) as the *error correlation* matrix.

C. Posterior Cramér-Rao bound

The PCRb [27] provides an estimator-agnostic lower bound to the estimation error (2). More importantly for us, PCRb sets a lower limit on the estimator MSE in the sense that the difference between the expected mean square error correlation matrix and a matrix determined by the model of the estimation problem is positive semidefinite [8]. Consider the sequence of states and measurements until time k : $\mathbf{x}_{0:k} = (\mathbf{x}_0, \mathbf{x}_1, \dots, \mathbf{x}_k)$, $\mathbf{y}_{1:k} = (\mathbf{y}_1, \dots, \mathbf{y}_k)$. The joint distribution over the state and measurements based on (1) is

$$p(\mathbf{x}_{0:k}, \mathbf{y}_{1:k} | \theta) = p(\mathbf{x}_0) \prod_{i=0}^{k-1} p(\mathbf{x}_{i+1} | \mathbf{x}_i, \theta) \prod_{j=1}^k p(\mathbf{y}_j | \mathbf{x}_j, \theta)$$

where θ represents sensor parameters that we want to identify. The PCRb on the estimation error is

$$\begin{aligned} \mathbf{P}_{\mathbf{x}_{0:k}}(\theta) &\triangleq \mathbb{E} \left[(g(\mathbf{y}_{1:k}) - \mathbf{x}_{0:k})(g(\mathbf{y}_{1:k}) - \mathbf{x}_{0:k})^T \right] \\ &\succcurlyeq (\mathcal{I}_{\mathbf{x}_{0:k}}(\theta))^{-1}, \end{aligned}$$

where $\mathbf{P}_{\mathbf{x}_{0:k}}$ is the error correlation matrix associated with estimating $\mathbf{x}_{0:k}$ and

$$\mathcal{I}_{\mathbf{x}_{0:k}}(\theta) = \mathbb{E} \left[-\frac{\partial^2 \log p(\mathbf{x}_{0:k}, \mathbf{y}_{1:k} | \theta)}{\partial \mathbf{x}_{0:k} \partial \mathbf{x}_{0:k}^T} \right] \quad (3)$$

is the (Fisher) information matrix [6], [9]. Note that the information matrix is a function of the parameters θ .

IV. PROBLEM STATEMENT

We represent a sensor query schedule either by a sequence of monotonic time instants, $\mathbf{t}_s = (t_1, t_2, \dots)$, or as a single parameter, m_s , when the sensor is queried at a constant rate. The sensor covariance is represented by \mathbf{R} and the desired estimation accuracy by the positive scalar k_a .

The objectives of our works are (i) identify a sensor query schedule (for a given sensor covariance) with minimum entries in \mathbf{t}_s or the smallest m_s that achieves the desired estimation accuracy, and (ii) identify sensor covariances (for a given sensor query schedule) that achieve the desired estimation accuracy. We can express these objectives as the following optimization problem

$$\begin{aligned} \min_{\theta} \quad & s(\theta) \\ \text{s.t.} \quad & \text{MSE}(\mathbf{x}_{0:k}) \text{ is at most } k_a^2. \end{aligned} \quad (4)$$

where as before $s(\cdot)$ is a parameter-dependent function with $\theta = m_s$ or $\theta = \mathbf{R}$. In the next section, we develop a computationally tractable convex formulation for (4).

V. METHODOLOGY

A challenge associated (4) is that the MSE depends on a particular realization $g(\mathbf{y}_{1:k})$ of a specific estimator. In contrast, the FIM provides an estimator-independent lower bound to the estimator MSE. An alternative optimization problem that uses the FIM to estimate sensor parameters is as follows

$$\begin{aligned} \min_{\theta} \quad & s(\theta) \\ \text{s.t.} \quad & (\mathcal{I}_{\mathbf{x}_{0:k}}(\theta))^{-1} \text{ is at most } k_a^2, \end{aligned} \quad (5)$$

However, calculating the inverse of the FIM can be expensive. In the next section, we derive a recursive form for the PCRb that is computationally tractable and in the subsequent section we incorporate the desired estimation accuracy into the recursive PCRb.

A. Recursive posterior Cramér-Rao bound

Our objective in this section is to obtain a recursive form for the PCRb associated with the joint distribution $p(\mathbf{x}_{0:k}, \mathbf{y}_{1:k}, \mathbf{x}_{k+1} | \theta)$. For brevity, we denote the joint distribution $p(\mathbf{x}_{0:k}, \mathbf{y}_{1:k}, \mathbf{x}_{k+1} | \theta)$ by p_{k+1} . Let $\tilde{\mathcal{I}}_{\mathbf{x}_{0:k+1}}(\theta)$ be the information matrix derived from p_{k+1} . The *check* ($\check{\cdot}$) notation is used to indicate the information matrix associated with a predictive distribution, i.e., the information until time $k = n + 1$ excluding the observation \mathbf{y}_{k+1} . The PCRb for

a decomposed form of the error correlation matrix and the information matrix is

$$\begin{bmatrix} \check{\mathbf{P}}_{\mathbf{x}_{0:k}} & \check{\mathbf{P}}_{\mathbf{x}_{0:k}, \mathbf{x}_{k+1}} \\ \check{\mathbf{P}}_{\mathbf{x}_{k+1}, \mathbf{x}_{0:k}} & \check{\mathbf{P}}_{\mathbf{x}_{k+1}} \end{bmatrix} \succcurlyeq \begin{bmatrix} \mathbf{A}_{k+1} & \mathbf{B}_{k+1} \\ \mathbf{B}_{k+1}^T & \mathbf{C}_{k+1} \end{bmatrix}^{-1},$$

where the dependency on θ has been omitted for brevity, $\check{\mathbf{P}}_{\mathbf{x}_{0:k}}$ and $\check{\mathbf{P}}_{\mathbf{x}_{k+1}}$ are the error correlation submatrices associated with $\mathbf{x}_{0:k}$ and \mathbf{x}_{k+1} , respectively, $\check{\mathbf{P}}_{\mathbf{x}_{0:k}, \mathbf{x}_{k+1}}$ is the error cross-correlation submatrix, and

$$\mathbf{A}_{k+1} = \mathbb{E} \left[-\frac{\partial^2 \log p_{k+1}}{\partial \mathbf{x}_{0:k} \partial \mathbf{x}_{0:k}^T} \right], \mathbf{B}_{k+1} = \mathbb{E} \left[-\frac{\partial^2 \log p_{k+1}}{\partial \mathbf{x}_{0:k} \partial \mathbf{x}_{k+1}^T} \right],$$

$$\mathbf{B}_{k+1}^T = \mathbb{E} \left[-\frac{\partial^2 \log p_{k+1}}{\partial \mathbf{x}_{k+1} \partial \mathbf{x}_{0:k}^T} \right], \mathbf{C}_{k+1} = \mathbb{E} \left[-\frac{\partial^2 \log p_{k+1}}{\partial \mathbf{x}_{k+1} \partial \mathbf{x}_{k+1}^T} \right].$$

As noted in [5], the estimation error associated with \mathbf{x}_{k+1} is lower bounded by the inverse of the right-lower block of $(\check{\mathbf{J}}_{\mathbf{x}_{0:k+1}}(\theta))^{-1}$, denoted here by $\check{\mathbf{J}}_{\mathbf{x}_{k+1}}$:

$$\check{\mathbf{P}}_{\mathbf{x}_{k+1}} \succcurlyeq (\check{\mathbf{J}}_{\mathbf{x}_{k+1}})^{-1} \triangleq \mathbf{C}_{k+1} - \mathbf{B}_{k+1}^T \mathbf{A}_{k+1}^{-1} \mathbf{B}_{k+1}. \quad (6)$$

However, (6) requires inverting a relatively large \mathbf{A}_{k+1} , which is expensive. The following proposition gives a recursive form that is computationally more efficient.

Proposition 1. *Let $\check{\mathbf{x}}_{k+1}$ be the one-step-ahead predictor for \mathbf{x}_{k+1} . The correlation matrix of estimation error $\check{\mathbf{P}}_{\mathbf{x}_{k+1}} = \mathbb{E} [(\check{\mathbf{x}}_{k+1} - \mathbf{x}_{k+1})(\check{\mathbf{x}}_{k+1} - \mathbf{x}_{k+1})^T]$ is lower bounded by matrix $\check{\mathbf{J}}_{\mathbf{x}_{k+1}}$ for any time $k = 0, 1, 2, \dots$:*

$$\check{\mathbf{P}}_{\mathbf{x}_{k+1}} \succcurlyeq (\check{\mathbf{J}}_{\mathbf{x}_{k+1}})^{-1}, \quad (7)$$

where $\check{\mathbf{J}}_{\mathbf{x}_{k+1}}$ obeys the recursion

$$\check{\mathbf{J}}_{\mathbf{x}_{k+1}} = \mathbf{D}_{k+1}^{22} - \mathbf{D}_{k+1}^{21} (\mathbf{D}_{k+1}^{11} + \check{\mathbf{J}}_{\mathbf{x}_k})^{-1} \mathbf{D}_{k+1}^{12} \quad (8)$$

with

$$\mathbf{D}_{k+1}^{11} = \mathbb{E} \left[-\frac{\partial^2 \log p(\mathbf{x}_{k+1} | \mathbf{x}_k)}{\partial \mathbf{x}_k \partial \mathbf{x}_k^T} - \frac{\partial^2 \log p(\mathbf{y}_k | \mathbf{x}_k)}{\partial \mathbf{x}_k \partial \mathbf{x}_k^T} \right],$$

$$\mathbf{D}_{k+1}^{12} = \mathbb{E} \left[-\frac{\partial^2 \log p(\mathbf{x}_{k+1} | \mathbf{x}_k)}{\partial \mathbf{x}_k \partial \mathbf{x}_{k+1}^T} \right], \quad \mathbf{D}_{k+1}^{21} = (\mathbf{D}_{k+1}^{12})^T,$$

$$\mathbf{D}_{k+1}^{22} = \mathbb{E} \left[-\frac{\partial^2 \log p(\mathbf{x}_{k+1} | \mathbf{x}_k)}{\partial \mathbf{x}_{k+1} \partial \mathbf{x}_{k+1}^T} \right].$$

The recursion is initiated by $\check{\mathbf{J}}_{\mathbf{x}_0} = \mathbb{E} \left[-\frac{\partial^2 \log p(\mathbf{x}_0)}{\partial \mathbf{x}_0 \partial \mathbf{x}_0^T} \right]$. The statement holds under the additional assumption that the relevant derivatives, expectations, and matrix inversions exist.

Proof. The result follows the same argument as [5, Proposition 1] applied to the prediction step, instead of the update step, of the filter. \square

Although the Hessians in (8) look complicated, they simplify for the system (1) under the AWGN assumption:

$$\mathbf{D}_{k+1}^{11} = \mathbb{E} [\mathbf{F}_k^T \mathbf{Q}_k^{-1} \mathbf{F}_k] + \mathbb{E} [\mathbf{H}_k^T \mathbf{R}^{-1} \mathbf{H}_k], \quad (9)$$

$$\mathbf{D}_{k+1}^{12} = -\mathbb{E} [\mathbf{F}_k] \mathbf{Q}_k^{-1}, \quad \mathbf{D}_{k+1}^{22} = \mathbf{Q}_k^{-1},$$

where

$$\mathbf{F}_k = \frac{\partial \mathbf{f}(\mathbf{x}_k)}{\partial \mathbf{x}_k}, \quad \mathbf{H}_k = \frac{\partial \mathbf{h}(\mathbf{x}_k)}{\partial \mathbf{x}_k}.$$

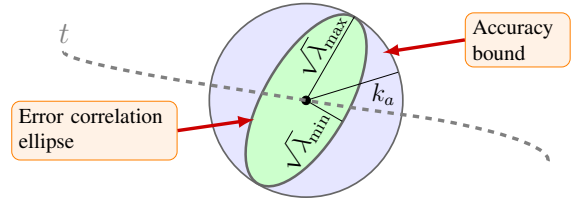


Fig. 2. The error correlation matrix, $\check{\mathbf{P}}_{\mathbf{x}_t}$, viewed as the ellipse $\{\mathbf{x} \in \mathbb{R}^2 \mid \mathbf{x}^T (\check{\mathbf{P}}_{\mathbf{x}_t})^{-1} \mathbf{x} \leq 1\}$ (green), represents the spread of errors and the square root of its maximum eigenvalue, λ_{\max} , gives the maximum error along any principle axis. To achieve desired accuracy k_a , the error ellipse must be within the accuracy bound ellipse $\{\mathbf{x} \in \mathbb{R}^2 \mid \mathbf{x}^T (k_a^2 \mathbf{I})^{-1} \mathbf{x} \leq 1\}$ (blue) at each time step t (gray dashed line).

The expectations can be computed using Monte Carlo methods or Gaussian quadrature. The upshot is that we now have a way to recursively compute a lower bound to the estimation error at each time step.

B. Constraint on estimation error

In this section, we take the required estimation accuracy into account by incorporating it as a constraint on the information submatrix $\check{\mathbf{J}}_{\mathbf{x}_{k+1}}$. We begin by noting that the square root of the eigenvalues of the error correlation matrix $\check{\mathbf{P}}_{\mathbf{x}_{k+1}}$ represent the magnitude of the spread of estimation error along principle directions (given by eigenvectors), with the square root of the maximum eigenvalue, $\sqrt{\lambda_{\max}(\check{\mathbf{P}}_{\mathbf{x}_{k+1}})}$, representing the maximum spread of estimation error in any direction (see Figure 2). To achieve the necessary accuracy, we require that the square root of the maximum eigenvalue of the error correlation matrix is at most the required accuracy:

$$\lambda_{\max}(\check{\mathbf{P}}_{\mathbf{x}_{k+1}}) \leq k_a^2. \quad (10)$$

The above inequality can also be expressed by the following convex constraint [28, Appendix A.5.2]

$$\check{\mathbf{P}}_{\mathbf{x}_{k+1}} \preceq k_a^2 \mathbf{I}, \quad (11)$$

where \mathbf{I} is the identity matrix. We can obtain a constraint on the information submatrix from (7) and (11) as

$$\check{\mathbf{J}}_{\mathbf{x}_{k+1}} \succcurlyeq (\check{\mathbf{P}}_{\mathbf{x}_{k+1}})^{-1} \succcurlyeq k_a^{-2} \mathbf{I}. \quad (12)$$

Including the recursion from (8) in the above inequality gives the following relation

$$\mathbf{D}_{k+1}^{22} - \mathbf{D}_{k+1}^{21} (\mathbf{D}_{k+1}^{11} + \check{\mathbf{J}}_{\mathbf{x}_k})^{-1} \mathbf{D}_{k+1}^{12} \succcurlyeq k_a^{-2} \mathbf{I}.$$

Moving $k_a^{-2} \mathbf{I}$ to the left side and using the Schur complement characterization of symmetric positive semidefinite matrices [29, Proposition 2.2], we get the following conic inequality constraint

$$\mathbf{S}_k(\theta) \triangleq \begin{bmatrix} \check{\mathbf{J}}_{\mathbf{x}_k} + \mathbf{D}_{k+1}^{11} & \mathbf{D}_{k+1}^{12} \\ \mathbf{D}_{k+1}^{21} & \mathbf{D}_{k+1}^{22} - k_a^{-2} \mathbf{I} \end{bmatrix} \succcurlyeq 0. \quad (13)$$

C. Optimization problem

We now present the main result of our work. As outlined in Section IV, our objective is to identify sensor parameters to achieve a pre-specified estimation accuracy. To achieve the necessary estimation accuracy, (13) outlines the constraint that

must be satisfied. Any parameter that satisfies (13) is a feasible parameter. As such, we can cast the problem of identifying optimal parameters at each time step $k = 0, 1, \dots$ as solving the following optimization problem

$$\begin{aligned} \min_{\theta} \quad & s(\theta) \\ \text{s.t.} \quad & \mathbf{S}_k(\theta) \succcurlyeq 0. \end{aligned} \quad (14)$$

where as before $s(\cdot)$ is a parameter-dependent function. The parameter θ can be constant or change over time. The optimization problem (14) is general and can be used in any setup that satisfies the assumptions outlined in Section IV. In the next section, we apply it to the calculation of sensor query schedules and sensor covariances for estimating the trajectory of a mobile robot to the desired accuracy.

VI. TRAJECTORY ESTIMATION

Our approach in this section is as follows: First, we present expressions for the process model Jacobian, \mathbf{F}_k , the measurement model Jacobian, \mathbf{H}_k , and the covariance function, \mathbf{Q}_k , that are required for formulating the constraint (13). Next, we use this constraint in (14) to solve for sensor query schedules and sensor covariances. We use the framework of continuous-time trajectory estimation [30], [31] that uses a continuous-time motion model and discrete-time measurement models. We use a continuous-time motion model as the state and the corresponding uncertainty can be computed at arbitrary time instants, which is ideal for scheduling measurements.

A. Motion model

We use a *white noise on velocity* (WNOV) or a constant-velocity motion model as the system process model. Specifically, we use motion priors based on linear time-invariant stochastic differential equations:

$$\dot{\mathbf{x}}(t) = \mathbf{u}(t) + \mathbf{w}(t), \quad (15)$$

where $\mathbf{x}(t) \in \mathbb{R}^d$ is the state and $\dot{\mathbf{x}}(t)$ is the corresponding time derivative, $\mathbf{u}(t) \in \mathbb{R}^d$ is the velocity input, and $\mathbf{w}(t) \sim \mathcal{GP}(0, \mathbf{Q}\delta(t-t'))$ is a zero-mean Gaussian Process (GP) with power spectral density matrix \mathbf{Q} . The state consists of the robot's position, $\mathbf{x}(t) = \mathbf{p}(t)$, however, the procedure outlined here can be applied to nonlinear spaces such as the special Euclidean ($SE(d)$) manifold using local poses defined on vector spaces [32]. The mean of the GP prior between two consecutive time instants t_k and t_{k+1} is

$$\mathbf{x}_{k+1} = \mathbf{x}_k + \mathbf{u}_k \Delta t_k, \quad (16)$$

where $\mathbf{x}_k = \mathbf{x}(t_k)$ and $\Delta t_k = t_{k+1} - t_k$. The process model Jacobian and the covariance function are [31, Section 3.4]:

$$\mathbf{F}_k = \mathbf{I}, \quad \mathbf{Q}_k = \mathbf{Q} \Delta t_k. \quad (17)$$

B. Measurement models

In this section, we present measurement models and Jacobians for two commonly used sensing modalities: *position* and *range* sensors.

1) *Position measurement model*: The observations in this case are the position of the mobile robot over time:

$$\tilde{\mathbf{p}}_k = \mathbf{x}_k + \boldsymbol{\eta}_{p_k}, \quad (18)$$

where $\tilde{\mathbf{p}}_k \in \mathbb{R}^d$ is a measurement of the true position $\mathbf{x}_k \in \mathbb{R}^d$ at time k and $\boldsymbol{\eta}_{p_k} \sim \mathcal{N}(0, \mathbf{R}_{p_k})$ is AWGN of covariance \mathbf{R}_{p_k} . The measurement Jacobian in this case is $\mathbf{H}_{p_k} = \mathbf{I}$.

2) *Range measurement model*: In range-based localization, the measurement model consists of the distance measured between a tag and an anchor:

$$r_{a_k} = \|\mathbf{p}_a - \mathbf{x}_k\|_2 + \eta_{r_k}, \quad (19)$$

where $r_{a_k} \in \mathbb{R}$ is the measured distance to anchor a with position $\mathbf{p}_a \in \mathbb{R}^d$, $\|\cdot\|_2$ is the L_2 norm, and $\eta_{r_k} \sim \mathcal{N}(0, \sigma_{r_k}^2)$ is AWGN of variance $\sigma_{r_k}^2$. Commonly used technologies for range-based positioning include WiFi, UWB, sonar, radar, and lidar. The corresponding measurement Jacobian is

$$\mathbf{H}_{r_k} = -\frac{(\mathbf{p}_a - \mathbf{x}_k)^T}{\|\mathbf{p}_a - \mathbf{x}_k\|_2}. \quad (20)$$

We now have the necessary components to apply our optimization problem (14) to trajectory estimation for determining required parameters.

C. Parameter estimation

1) *Sensor query schedule estimation*: As mentioned in Section IV, we want to identify a sensor query schedule that minimizes the number of queries. For a given trajectory duration, this is equivalent to maximizing the duration between subsequent measurement times (see Figure 1). If we consider t_k and t_{k+1} to be aligned with successive measurements and as such with consecutive sensor queries, then Δt_k from (16) corresponds to the time duration between subsequent sensor queries. Substituting expressions for the process model Jacobian and the covariance function from (17) in (13), we get the following optimization problem

$$\begin{aligned} \max_{\Delta t_k \in \mathbb{R}_{++}} \quad & \Delta t_k \\ \text{s.t.} \quad & \mathbf{S}_k(\Delta t_k) \succcurlyeq 0, \quad k = 0, 1, 2, \dots \end{aligned} \quad (21)$$

where

$$\mathbf{S}_k(\Delta t_k) = \begin{bmatrix} \check{\mathbf{J}}_{\mathbf{x}_k} + \mathbf{Q}_k^{-1} + \mathbb{E}[\mathbf{H}_k^T \mathbf{R}_k^{-1} \mathbf{H}_k] & \mathbf{Q}_k^{-1} \\ \mathbf{Q}_k^{-1} & \mathbf{Q}_k^{-1} - k_a^{-2} \mathbf{I} \end{bmatrix} \succcurlyeq 0$$

with $\mathbf{Q}_k = \mathbf{Q} \Delta t_k$. According to the principles of disciplined convex programming [33], (21) is not convex in Δt_k , however, it is convex in Δt_k^{-1} . We can reformulate the above problem as a convex problem by setting $m_k = \Delta t_k^{-1}$:

$$\begin{aligned} \min_{m_k \in \mathbb{R}_{++}} \quad & m_k \\ \text{s.t.} \quad & \mathbf{S}_k(m_k) \succcurlyeq 0, \quad k = 0, 1, 2, \dots \end{aligned} \quad (22)$$

where

$$\mathbf{S}_k(m_k) = \begin{bmatrix} \check{\mathbf{J}}_{\mathbf{x}_k} + \mathbf{Q}_{m_k}^{-1} + \mathbb{E}[\mathbf{H}_k^T \mathbf{R}_k^{-1} \mathbf{H}_k] & \mathbf{Q}_{m_k}^{-1} \\ \mathbf{Q}_{m_k}^{-1} & \mathbf{Q}_{m_k}^{-1} - k_a^{-2} \mathbf{I} \end{bmatrix},$$

with $\mathbf{Q}_{m_k} = \mathbf{Q} m_k^{-1}$. For the WNOV motion model (15), the inequality constraint in (22) is a linear matrix inequality (LMI) at each time step and consequently (22) is a semidefinite

program (SDP). We can initialize the recursion for (22) by (i) setting $\check{\mathbf{J}}_{\mathbf{x}_0} = \mathbb{E} \left[-\frac{\partial^2 \log p(\mathbf{x}_0)}{\partial \mathbf{x}_0 \partial \mathbf{x}_0^T} \right]$ if the distribution over the initial state, $p(\mathbf{x}_0)$, is known, or (ii) setting $\check{\mathbf{J}}_{\mathbf{x}_0} = k_a^2 \mathbf{I}$ if the initial state is known. Once Δt_k is computed, $\check{\mathbf{J}}_{\mathbf{x}_{k+1}}$ can be computed using (8) for the next iteration.

For robots operating in uniform conditions, we can obtain nominal values for Jacobians. Assuming the initial conditions are known, we can solve for a constant sensor query rate:

$$\begin{aligned} \min_{m_s \in \mathbb{R}_{++}} \quad & m_s \\ \text{s.t.} \quad & \mathbf{S}(m_s) \succcurlyeq 0, \end{aligned} \quad (23)$$

where

$$\mathbf{S}(m_s) = \begin{bmatrix} \check{\mathbf{J}}_{\mathbf{x}_k} + \mathbf{Q}_{m_s}^{-1} + \mathbb{E} [\mathbf{H}_k^T \mathbf{R}_k^{-1} \mathbf{H}_k] & \\ & \mathbf{Q}_{m_s}^{-1} - k_a^{-2} \mathbf{I} \end{bmatrix},$$

with $\mathbf{Q}_{m_s} = \mathbf{Q} m_s^{-1}$ and $\check{\mathbf{J}}_{\mathbf{x}_k} = k_a^{-2} \mathbf{I}$, since we are solving for a constant sensor query rate. Nominal value for a measurement Jacobian depends on the sensing modality. For instance, for a position sensor, we have $\mathbf{H}_k = \mathbf{H} = \mathbf{I}$.

2) *Sensor covariance estimation*: In this section, we want to identify a sensor covariance matrix to achieve a desired accuracy for a given sensor query schedule. We use \mathbf{R} to refer to both \mathbf{R}_p for position sensor covariance and σ_r^2 for range sensor covariance. Similar to the previous case, (13) is not convex in \mathbf{R}_k but is convex in \mathbf{R}_k^{-1} . The optimization problem (14) in this case is

$$\begin{aligned} \min_{\mathbf{R}_k^{-1} \in \mathbb{S}_{++}^d} \quad & \text{tr}(\mathbf{R}_k^{-1}) \\ \text{s.t.} \quad & \mathbf{S}_k(\mathbf{R}_k^{-1}) \succcurlyeq 0, \quad k = 0, 1, 2, \dots \end{aligned} \quad (24)$$

where $\text{tr}(\mathbf{A})$ is the trace of matrix \mathbf{A} and

$$\mathbf{S}_k(\mathbf{R}_k^{-1}) = \begin{bmatrix} \check{\mathbf{J}}_{\mathbf{x}_k} + \mathbf{Q}_k^{-1} + \mathbb{E} [\mathbf{H}_k^T \mathbf{R}_k^{-1} \mathbf{H}_k] & \\ & \mathbf{Q}_k^{-1} - k_a^{-2} \mathbf{I} \end{bmatrix}.$$

We chose to minimize the trace of the inverse covariance matrix, which corresponds to the A -optimal design criteria [28, Section 7.5.2]. However, other design criteria, such as minimizing the determinant (D -optimal) or minimizing the norm (E -optimal) of \mathbf{R}_k^{-1} can be used while retaining convexity. In (24), we solve for a different measurement covariance at each time instant. Alternatively, we can optimize for a constant measurement covariance for uniform trajectories.

Remark 1. *When using sensing modalities with lower dimensionality compared to the state, multiple measurements are needed if $\check{\mathbf{J}}_k \preccurlyeq k_a^{-2} \mathbf{I}$. This is expected since a single lower-dimensional measurement cannot constrain the full state. For instance, in 2D trajectory estimation with range sensors, we require at least two anchors to calculate the Jacobian \mathbf{H}_k .*

VII. EXPERIMENTS

In this section, we apply our proposed methods to trajectory estimation in simulation and real experiments. We use the CVXPY [34] package with MOSEK [35] solver to optimize SDPs for identifying parameters and use Gaussian quadrature to calculate the necessary expectations. We estimate the trajectory of the robot using nonlinear batch maximum a posteriori (MAP) inference. We evaluate the performance of

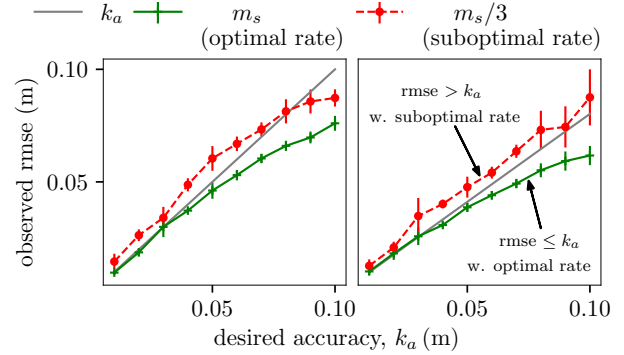


Fig. 3. Trajectory estimation results from simulation using position sensors (left) and range sensors (right) with different sensor query rates. Noise values for the position and the range sensors are $\sigma_p = 0.08$ m and $\sigma_r = 0.08$ m, respectively. The desired RMSE for a given accuracy value, k_a , is indicated by the black line in each case. RMSE values obtained using the proposed optimal sensor query rate, m_s (optimal rate), are equal to or lower than the desired accuracy k_a (black line), whereas the lower sensor query rate, $m_s/3$ (suboptimal rate), results in higher RMSE, indicating the validity of the proposed sensor query rate.

MAP inference using root-mean-squared error (RMSE) metric: $\|\mathbf{x}_{\text{gt}}(t) - \mathbf{x}_{\text{est}}(t)\|_2$, where $\mathbf{x}_{\text{gt}}(t)$ and $\mathbf{x}_{\text{est}}(t)$ are the true and the estimated states, respectively.

A. Simulation

1) *Sensor query schedule estimation*: The objective of this simulation is to show that for given sensor covariances, our proposed sensor query schedule achieves the required estimation accuracy. Our approach in simulation is as follows. We first sample random initial positions and velocities between $[-4, 4]$ m and $[-1, 1]$ m/s, respectively. The initial positions and velocities are used to generate a GP prior by simulating the system dynamics using (16). A ground-truth trajectory is generated by sampling uniformly from the GP prior. The process noise and sensor covariances are selected to reflect real systems and are constant across different experiments: $\mathbf{Q} = 0.001 \mathbf{I}$, $\mathbf{R}_p = 0.0064 \mathbf{I}$, and $\sigma_r^2 = 0.0064$. For each generated ground-truth trajectory, we calculate a constant sensor query schedule, m_s , using (23) for each $k_a \in [0.01, 0.1]$ m. In this case, the SDP state size is one (a single scalar) and the average time taken to solve for a constant sensor query rate in (23) is 0.017 s. Next, we simulate measurements according to the estimated sensor query schedule. These measurements are subsequently used in the MAP inference to estimate the robot trajectory. The estimated trajectory is compared with the ground trajectory to calculate the associated RMSE.

Average RMSE from 10 trials for each value of k_a for position and range sensors are shown in Figure 3. Error values for a query rate lower than the estimated rate, $m_s/3$, are also shown. In each case, the proposed sensor schedule achieves equal or lower error than the required accuracy and with query rate lower than the identified value, the estimation error is higher than the required accuracy in most cases. However, for $k_a > \sigma_r$ the estimated query schedule is conservative in some cases, indicating that a sensor query schedule with lower query rate could also be viable.

2) *Sensor covariance estimation*: In this section, our objective is to show that for a given sensor schedule, our proposed

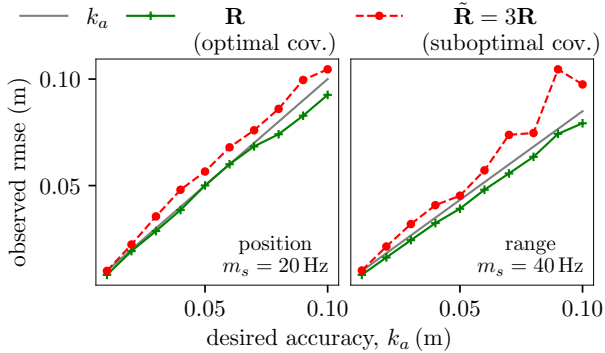


Fig. 4. Trajectory estimation results from simulation using position sensors (left) and range sensors (right) of proposed covariance, \mathbf{R} (optimal cov.), and higher covariance, $\hat{\mathbf{R}} = 3\mathbf{R}$ (suboptimal cov.). The desired RMSE for a given accuracy value, k_a , is indicated by the black line in each case. Using sensors with the proposed covariances, the trajectory estimation RMSE is lower than the desired accuracy k_a in each case. However, using sensors with higher covariances results in RMSE higher than the required accuracy, indicating the validity of our approach.

method estimates appropriate sensor covariances to achieve a certain estimation accuracy.

The setup for this case is similar to the previous case, but now we assume that the sensor covariances are unknown and a sensor query schedule is given. Specifically, we set $m_s = 20$ Hz for positions sensors and $m_s = 40$ Hz for range sensors and for each $k_a \in [0.01, 0.1]$ m we compute the corresponding sensor covariance, \mathbf{R} , using (24). For 2D trajectory estimation, the state consists of a 2×2 matrix and the average time taken to solve (24) at each time step is 0.017 s. The estimated sensor covariances and the provided sensor schedule are used to simulate measurements that are then used for MAP inference. Results from 10 trials for the different sensing modalities are shown in Figure 4. As before, the identified sensor covariances achieve RMSE lower than the required accuracy. For validation, we also computed RMSE with sensor covariances higher than the one proposed by our methods: $\hat{\mathbf{R}} = 3\mathbf{R}$. With higher sensor covariance, the estimation error is larger than the required accuracy in most cases, indicating the efficacy of our proposed method.

B. Real experiments

In real experiments, we apply our proposed method to estimate the trajectory of an omnidirectional mobile robot (see Figure 1). The test space is equipped with a motion capture system for ground-truth pose and eight UWB anchors at the corners of the arena. The data rate of the ground-truth pose is 100 Hz, and that of range data is 50 Hz. We performed multiple experiments where the mobile robot was commanded along predefined trajectories, and the sensor data was recorded on the onboard computer for offline evaluation.

1) *Sensor query schedule estimation*: We use the commanded trajectory and sensor covariances to calculate a constant sensor query schedule. To simulate noisy position measurements, we corrupt the ground-truth position with Gaussian noise of variance $\mathbf{R}_p = 0.0064\mathbf{I}$. The covariance of UWB-based range measurements is calculated using ground truth as $\sigma_r^2 = 0.0049$. To emulate different sensor query rates, we (sub)sampled the recorded data. Average trajectory estimation

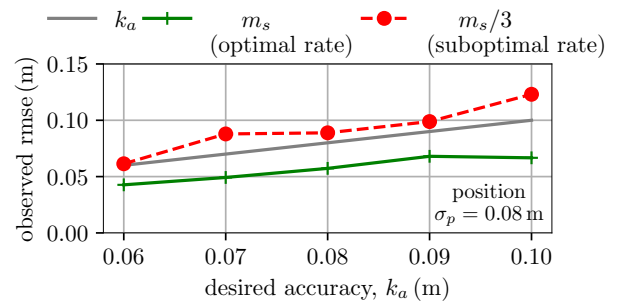


Fig. 5. Trajectory estimation RMSE from real experiments with position sensors sampled at the proposed sensor query rate, m_s (optimal rate), and a lower sensor query rate, $m_s/3$ (suboptimal rate). The desired RMSE for different accuracy values, k_a , is shown by the gray line. In all cases, the estimated sensor query rate yields RMSE equal to or lower than the desired accuracy k_a , whereas the lower sensor query rate results in higher RMSE.

RMSE from three experiments for $k_a \in [0.01, 0.1]$ m with position measurements and range measurements are shown in Figure 5 and in Table I, respectively. Estimated trajectories using range measurements from one such experiment are shown in Figure 1.

The results highlight the main benefits of our approach. Firstly, for feasible accuracy values, the estimated query rate achieves the desired performance, and a lower query rate, $m_s/3$, results in degraded performance, proving the validity of our approach. Secondly, our proposed method can be used to ascertain if specific accuracy is infeasible given the system parameters. For instance, with the process and sensor covariances in our real setup, the optimization problem for calculating the sensor query schedule for $k_a = 0.001$ m is infeasible (with a certificate of infeasibility from the numerical solver), providing feasible performance limits. Even with a feasible configuration, our approach can be used to identify operational limits. For example the recommended query rate for (i) $k_a = 0.03$ m with range sensors is 152 Hz and (ii) $k_a = 0.02$ m with position sensors is 340 Hz that are beyond the capabilities of the sensors used in our setup.

2) *Sensor covariance estimation*: As in simulation, the objective in this section is to estimate sensor covariances to achieve a certain estimation accuracy. We evaluate sensor covariance estimation for position sensors only, as results with range sensors are similar. The sensor query rate is set to $m_s = 20$ Hz for position sensors. Sensor data at the required query rate is generated by downsampling the recorded data. For each $k_a \in [0.01, 0.1]$ m, we compute the required sensor covariance \mathbf{R}_p using (24). To emulate noisy position sensors, AWGN with the estimated covariance is added to the down-sampled position data. Results from three trials for each value of k_a for the position sensors are shown in

TABLE I
TRAJECTORY ESTIMATION RMSE USING RANGE SENSORS FROM REAL EXPERIMENTS. THE PROPOSED SENSOR QUERY RATE, m_s , ACHIEVES RMSE VALUES LOWER THAN k_a AS DESIRED, WHEREAS THE SENSOR QUERY RATE, $m_s/3$ RESULTS IN RMSE VALUES LARGER THAN k_a .

Query frequency	RMSE (m)			
	$k_a = 0.07$ m	$k_a = 0.08$ m	$k_a = 0.09$ m	$k_a = 0.1$ m
m_s	0.055	0.054	0.067	0.092
$m_s/3$	0.072	0.155	0.171	0.156

TABLE II

TRAJECTORY ESTIMATION RMSE WITH POSITION SENSORS FROM REAL EXPERIMENTS. THE PROPOSED SENSOR COVARIANCE \mathbf{R}_p ACHIEVES RMSE VALUES LOWER THAN k_a AS DESIRED, WHEREAS THE SENSOR COVARIANCE $\tilde{\mathbf{R}}_p = 3\mathbf{R}_p$ RESULTS IN RMSE VALUES LARGER THAN k_a .

Sensor covariance	RMSE (m)			
	$k_a = 0.07$ m	$k_a = 0.08$ m	$k_a = 0.09$ m	$k_a = 0.1$ m
\mathbf{R}_p	0.049	0.064	0.074	0.0942
$\tilde{\mathbf{R}}_p = 3\mathbf{R}_p$	0.073	0.107	0.122	0.204

Figure II. For feasible parameter configurations, the identified sensor covariances achieve lower RMSE, and higher sensor covariances, $\tilde{\mathbf{R}}_p = 3\mathbf{R}_p$, achieve higher RMSE compared to the desired accuracy as shown in Table II, indicating the validity of our approach.

VIII. CONCLUSION AND FUTURE WORK

In this work, we presented a framework to estimate sensor parameters to achieve the desired estimation accuracy. We applied our method to calculate the sensor query schedules and the sensor covariances necessary to attain a desired trajectory estimation accuracy. We validated our approach in simulation and real experiments by showing that a desired trajectory estimation RMSE is achieved using the calculated sensor schedules and covariances. The proposed method also identifies scenarios where a certain RMSE is unachievable given the system and sensor parameters. There are several avenues to explore further, such as the inclusion of diverse motion models, estimation of process covariances, and extension to nonlinear manifolds.

REFERENCES

- [1] The implementation of two-way ranging with the DW1000. https://thetoolchain.com/mirror/dw1000/aps013_dw1000_and_two_way_ranging.pdf.
- [2] Anastasios I. Mourikis and Stergios I. Roumeliotis. Optimal sensor scheduling for resource-constrained localization of mobile robot formations. *IEEE Transactions on Robotics*, 22(5):917–931, 2006.
- [3] Valerio Magnago, Pablo Corbalan, Gian Pietro Picco, Luigi Palopoli, and Daniele Fontanelli. Robot localization via odometry-assisted ultra-wideband ranging with stochastic guarantees. In *Proc. of the International Conference on Intelligent Robots and Systems (IROS)*, pages 1607–1613. IEEE, 2019.
- [4] Qi Yan, Li Jiang, and Solmaz S. Kia. Measurement scheduling for cooperative localization in resource-constrained conditions. *IEEE Robotics and Automation Letters*, 5(2):1991–1998, 2020.
- [5] P. Tichavsky, C.H. Muravchik, and A. Nehorai. Posterior Cramér-Rao bounds for discrete-time nonlinear filtering. *IEEE Transactions on Signal Processing*, 46(5):1386–1396, May 1998.
- [6] C. Radhakrishna Rao. Information and the Accuracy Attainable in the Estimation of Statistical Parameters. *Bulletin of the Calcutta Mathematical Society*, 37:81–91, 1945.
- [7] Harald Cramér. *Mathematical methods of statistics*, volume 26. Princeton university press, 1946.
- [8] Niclas Bergman. Posterior Cramér-Rao Bounds for Sequential Estimation. In *Sequential Monte Carlo Methods in Practice*, chapter 15, pages 321–338. Springer New York, New York, NY, 2001.
- [9] R. A. Fisher. Theory of statistical estimation. *Mathematical Proceedings of the Cambridge Philosophical Society*, 22(5):700–725, 1925.
- [10] Zhan Wang and Gamini Disisanayake. Observability Analysis of SLAM Using Fisher Information Matrix. In *Proc. of the 10th International Conference on Control, Automation, Robotics and Vision*, pages 1242–1247, Hanoi, Vietnam, December 2008. IEEE.
- [11] Alan Papalia, Nicole Thumma, and John Leonard. Prioritized Planning for Cooperative Range-Only Localization in Multi-Robot Networks. In *Proc. of the International Conference on Robotics and Automation (ICRA)*, pages 10753–10759, Philadelphia, USA, May 2022. IEEE.
- [12] Zichao Zhang and Davide Scaramuzza. Beyond point clouds: Fisher information field for active visual localization. In *Proc. of the International Conference on Robotics and Automation (ICRA)*, volume 2019-May, pages 5986–5992, 2019.
- [13] Andrea Censi. On achievable accuracy for range-finder localization. In *Proc. of the International Conference on Robotics and Automation (ICRA)*, pages 4170–4175, Rome, Italy, April 2007. IEEE.
- [14] B. Yang and J. Scheuing. Cramér-Rao bound and optimum sensor array for source localization from time differences of arrival. *ICASSP, IEEE International Conference on Acoustics, Speech and Signal Processing - Proceedings*, IV(3):iv/961–iv/964 Vol. 4, 2005.
- [15] Wenda Zhao, Abhishek Goudar, and Angela P. Schoellig. Finding the right place: Sensor placement for UWB time difference of arrival localization in cluttered indoor environments. *IEEE Robotics and Automation Letters*, 7(3):6075–6082, 2022.
- [16] Andreas Krause and Carlos Guestrin. Near-optimal Observation Selection using Submodular Functions. *AAAI*, 7:1650–1654, 2007.
- [17] Andreas Krause, Rajagopal Ram, Anupam Gupta, and Carlos Guestrin. Simultaneous placement and scheduling of sensors. *International Conference on Information Processing in Sensor Networks*, pages 181–192, 2009.
- [18] Pushyami Kaveti, Matthew Giamou, Hanumant Singh, and David M. Rosen. OASIS: Optimal arrangements for sensing in SLAM. In *Proc. of the International Conference on Robotics and Automation (ICRA)*, pages 13818–13824. IEEE, 2024.
- [19] Ethan Sequeira, Hussein Saad, Stephen Kelly, and Matthew Giamou. Towards Optimal Beacon Placement for Range-Aided Localization. In *Proc. of the Conference on Robots and Vision*, May 2024.
- [20] M.L. Hernandez, T. Kirubarajan, and Y. Bar-Shalom. Multisensor resource deployment using posterior Cramér-Rao bounds. *IEEE Transactions on Aerospace and Electronic Systems*, 40(2):399–416, April 2004.
- [21] Daniel D. Selvaratnam, Iman Shames, Branko Ristic, and Jonathan H. Manton. The Effect of Sensor Modality on Posterior Cramér-Rao Bounds for Simultaneous Localisation and Mapping. *IFAC-PapersOnLine*, 49(15):242–247, 2016.
- [22] Jeremy N. Wong, David J. Yoon, Angela P. Schoellig, and Timothy D. Barfoot. Variational Inference with Parameter Learning Applied to Vehicle Trajectory Estimation. *IEEE Robotics and Automation Letters*, 5(4):5291–5298, 2020.
- [23] Jeremy N. Wong, David J. Yoon, Angela P. Schoellig, and Timothy D. Barfoot. A Data-Driven Motion Prior for Continuous-Time Trajectory Estimation on SE(3). *IEEE Robotics and Automation Letters*, 5(2):1429–1436, 2020.
- [24] Mohamad Qadri, Zachary Manchester, and Michael Kaess. Learning covariances for estimation with constrained bilevel optimization. In *Proc. of the International Conference on Robotics and Automation (ICRA)*, pages 15951–15957. IEEE, 2023.
- [25] Kasra Khosoussi and Iman Shames. Joint State and Noise Covariance Estimation. (arXiv:2502.04584), 2025.
- [26] Dennis D. Wackerly, William Mendenhall, and Richard L. Scheaffer. *Mathematical Statistics with Applications*. Thomson Higher Education, Belmont, CA, 7th edition, 2008.
- [27] Harry L Van Trees. *Detection, Estimation, and Modulation Theory, Part I: Detection, Estimation, and Linear Modulation Theory*. John Wiley & Sons, 1968.
- [28] Stephen Boyd and Lieven Vandenbergh. *Convex Optimization*. Cambridge University Press, 2004.
- [29] Jean Gallier and others. The Schur Complement and Symmetric Positive Semidefinite (and Definite) Matrices. *Penn. Engineering*, pages 1–12, 2010.
- [30] Timothy D. Barfoot, Chi Hay Tong, and Simo Särkkä. Batch Continuous-Time Trajectory Estimation as Exactly Sparse Gaussian Process Regression. *Robotics: Science and Systems*, 2014.
- [31] Timothy D. Barfoot. *State Estimation for Robotics: Second Edition*. Cambridge University Press, January 2024.
- [32] Sean Anderson and Timothy D. Barfoot. Full STEAM ahead: Exactly sparse Gaussian process regression for batch continuous-time trajectory estimation on SE(3). Number 3, pages 157–164. IEEE, 2015.
- [33] Michael Grant, Stephen Boyd, and Yinyu Ye. *Disciplined Convex Programming*, pages 155–210. Springer US, Boston, MA, 2006.
- [34] Steven Diamond and Stephen Boyd. CVXPY: a python-embedded modeling language for convex optimization. *The Journal of Machine Learning Research*, 17(1):2909–2913, January 2016.
- [35] MOSEK ApS. *The MOSEK optimization toolbox for Python manual. Version 10.0.*, 2023.